JOC The Journal of Organic Chemistry

Article

pubs.acs.org/joc

Pyridinium Boranephosphonate Modified DNA Oligonucleotides

Subhadeep Roy,[†] Sibasish Paul,[†] Mithun Roy,[‡] Rajen Kundu,[†] Luca Monfregola,[†] and Marvin H. Caruthers*[,†]

[†]Department of Chemistry and Biochemistry, University of Colorado, Boulder, Colorado 80303, United States

[‡]Department of Basic Sciences and Humanities, National Institute of Technology, Manipur, Langol, Imphal, 795004 Manipur, India

Supporting Information

ABSTRACT: The synthesis of previously unknown derivatives of boranephosphonate that contain amine substitutions at boron and the incorporation of these derivatives into the backbone of DNA oligonucleotides is described. These derivatives result from iodine-mediated replacement of one BH_3 hydride of a boranephosphonate linkage by pyridine, various substituted pyridines, other aromatic amines, and certain unsaturated amines. Oligonucleotides containing these backbone modifications show enhanced uptake, relative to unmodified DNA, in mammalian cells. The redox behavior of the boranephosphonate and pyridinium boranephosphonate conjugated linkages has also been studied.

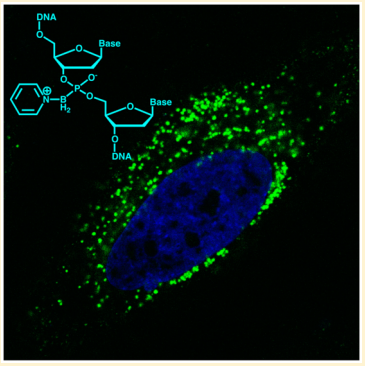

INTRODUCTION

Boranephosphonate diesters contain a borane group complexed to the phosphorus atom and demonstrate interesting chemical properties that have found applications in organophosphorus synthetic chemistry and material science. The B−P bond in these compounds is stable toward a wide range of conditions and reagents.[1] However, in the presence of strong oxidizing agents, the P−B bond can be activated to undergo a variety of reactions. Wada and co-workers have shown that in the presence of dimethoxytrityl cations under anhydrous conditions boranephosphonates can be converted to H-phosphonates.[2,3] We found that boranephosphonates reduce metals such as Au^{3+}, Pt^{2+}, and Ag^{+} to form nanoparticles.[4−6] More recently, we demonstrated that iodine can react with the borane group and activate it toward nucleophilic substitutions.[7] This reaction was used to produce DNA analogues containing a variety of substituents on the backbone phosphorus. Lastly, Ferry et al.[8] have used borane as a phosphorus protecting group during the synthesis of phostone mimetics of dissacharides. In all of these reactions, the oxidation of borane leads to a weakening of the P−B bond and subsequent reactions at the phosphorus center.

Here, we report a new reactivity of boranephosphonates where the substitution occurs at the boron atom. Specifically, we demonstrate that oxidation with iodine in the presence of certain amines leads to replacement of one hydride of borane with these amines. We further show that these derivatives can be prepared when boranephosphonate is part of a DNA backbone and that these modified deoxyoligonucleotides demonstrate enhanced uptake, relative to DNA in HeLa cells. Finally, investigations into the reductive properties of these compounds show that substitution at borane leads to a lower oxidative potential than the parent boranephosphonates.

RESULTS AND DISCUSSION

Synthesis of Pyridinium Boranephosphonate Nucleotides and Dinucleotides. Previously, we reported that, upon activation by iodine, boranephosphonates undergo a nucleophilic substitution at the phosphorus atom.[7] When we attempted to use this reactivity to form an internucleotide linkage through a reaction between 3′-*O*-boranephosphonate 5′-*O*-dimethoxytrityl-2′-deoxythymidine (**1**) and 3′-*O*-acetyl-2′-deoxythymidine in pyridine as solvent, the expected dinucleotide did not form. Instead, the ^{31}P NMR of this reaction mixture revealed that the resonance corresponding to **1** at 94 ppm had vanished while a new resonance at 63 ppm had appeared (Figure 1). The broad nature of this peak indicated that the P−B bond was intact. Purification of this compound by silica gel chromatography and analysis by ^{1}H NMR revealed that, in addition to the expected resonances corresponding to 2′-deoxyribose, thymine, and dimethoxytrityl, signals at 7.8, 8.3, and 8.8 ppm were present (Figure S1). These peaks correspond very well with those of pyridine. An additional 78 amu with respect to the starting material, **1**, in the mass spectrum of this compound confirmed the addition of a pyridine group and the concomitant loss of a hydrogen atom (Figure S3). Moreover the observed shift in the ^{11}B NMR spectrum (Figure 1C) hinted that the reaction had occurred at the boron center. We ascertained this by repeating the reaction with a boranephosphonate containing

Received: October 27, 2016
Published: January 18, 2017

DOI: 10.1021/acs.joc.6b02599
J. Org. Chem. 2017, 82, 1420−1427

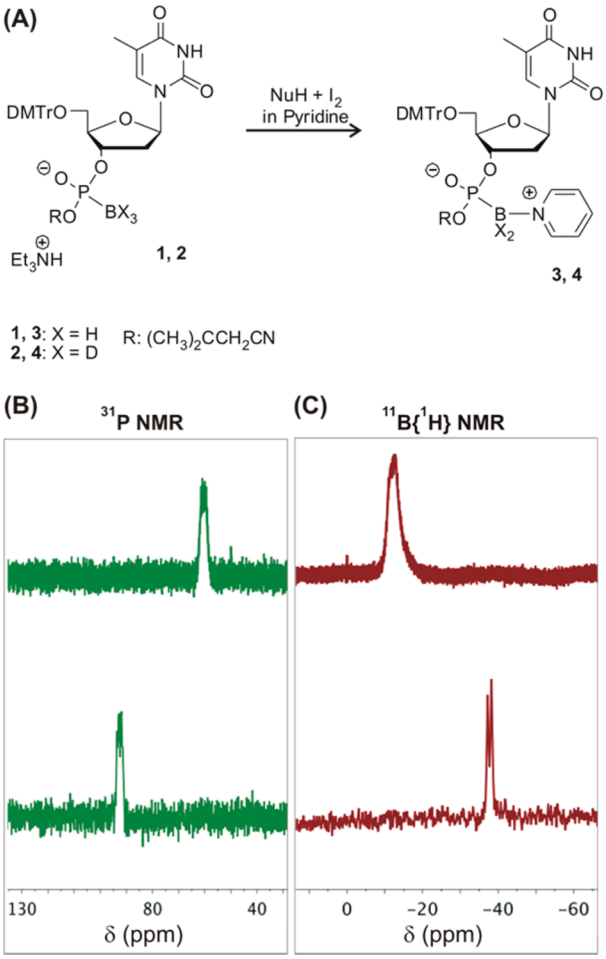

Figure 1. (A) Reaction of boranephosphonate diesters with pyridine upon activation by iodine. (B, C) Comparison of the ^{31}P and ^{11}B NMR spectra, respectively, of the starting material and the product. In each case, the bottom spectrum corresponds to the starting material (**1**) and the top spectrum to the product (**3**).

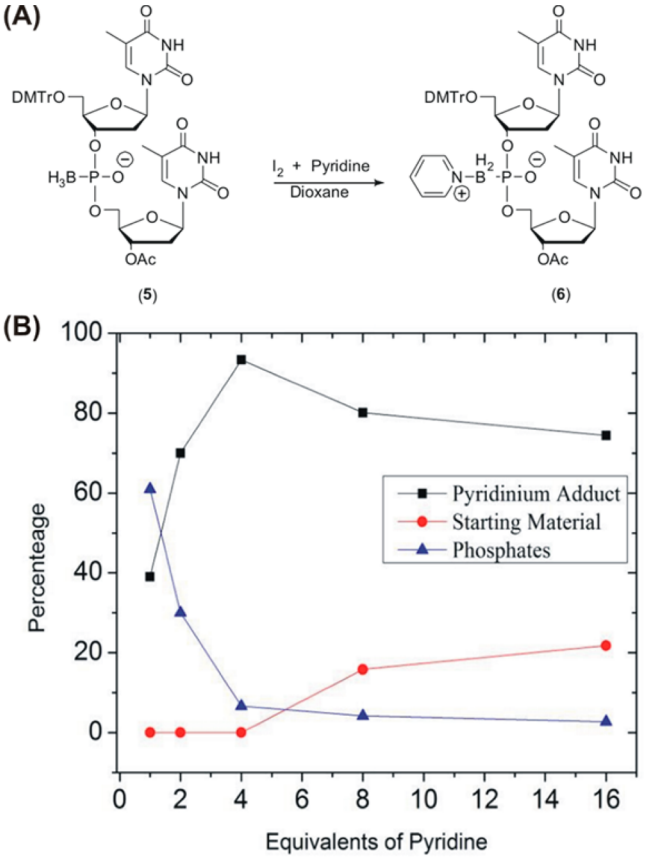

Figure 2. (A) Reaction of dithymidine boranephosphonate with pyridine activated by iodine. (B) Different products resulting from the reaction as a function of the amount of pyridine added. The graph shows the results 48 h from the start of the reaction.

BD_3 (**2**). The product in this case revealed an additional 77 amu, in accordance with the addition of a pyridine along with the loss of a deuterium atom (2 amu) (Figure S4). Based on these observations, we assigned the structures (**3**, **4**) shown in Figure 1A. Such structures are consistent with a previous report[9] of borane derivatives having the structure (pyridine)-$BH_2(PR_3)$.

In order to gain insight into a possible mechanism, we studied this reaction by varying the amounts of iodine and pyridine relative to the boranephosphonate diester substrate, by using pyridine derivatives of different steric and electronic properties, and by varying the iodinium source. With an eye toward utilizing this reactivity for introducing modifications into the DNA backbone, these experiments were carried out using dithymidine boranephosphonate (**5**) (Figure 2A) as the substrate. Reactions were monitored using ^{31}P NMR. We found that only a stoichiometric amount of iodine was necessary for near-quantitative yield of the product. However, more complex effects were observed upon varying the amount of pyridine (Figure 2B; full spectra are presented in Figure S14). At high relative amounts of pyridine, the pyridinium boranephosphonate was the only product formed, but the rate of reaction was slow and some starting material was still present after 48 h. In contrast, at close to stoichiometric amounts of pyridine with respect to **5**, hydrolyzed products such as the phosphate diester (with ^{31}P resonances around 0 ppm) were seen in addition to the desired product. We also discovered that *N*-iodosuccinimide (NIS) in place of iodine (I_2) as the source of the iodinium species led to both faster reaction rates and cleaner conversions to **6**. Based on these experiments, we observed that 3.0 equiv of *N*-iodosuccinimide and 10.0 equiv of pyridine in dioxane gave complete conversion to product within 15 min, without formation of side products.

Using NIS and dioxane as solvent, we next studied the reaction of **5** with various pyridine derivatives (added at a 10-fold excess over **5**, Table 1). Reactions occurred efficiently under these conditions with a number of substrates (as estimated by ^{31}P NMR after 24 h reaction). These include substrates having electron-withdrawing para substituents (4-trifluoromethylpyridine, Table 1, entry 5) as well as derivatives with an expanded aromatic system (4-methylquinoline, Table 1, entry 6). However, derivatives with bulky substituents at the 2 and 6 positions of pyridine (e.g., 2,6-dimethylpyridine or 2,6-di-*tert*-butylpyridine) remained recalcitrant toward this reaction even with NIS (Figure S15). We found that other aromatic amines such as *N*-methylimidazole (Table 1, entry 8) also formed similar products. We isolated and characterized compounds **6**, **11**, and **13**. In **13**, the presence of two nitrogens in *N*-methylimidazole raises the possibility of the reaction occurring at either center. While it is not possible to definitively assign structures based on our

DOI: 10.1021/acs.joc.6b02599
J. Org. Chem. 2017, 82, 1420−1427

Table 1. N-Iodosuccinamide Activated Substitution of Boranephosphonate Dimers (5) by Tertiary Amines*

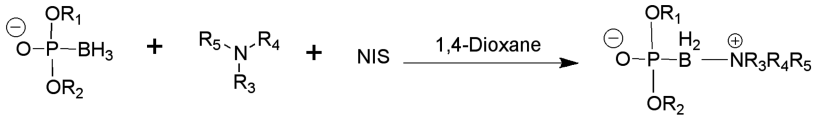

Entry	Amines	^{31}P NMR (ppm)	ESI$^+$ (m/z)	
			Observed	Theoretical
1.		60.29-62.68 (**6**)	966.3503[b]	966.3498
2.		61.95-62.16 (**7**)	1073.4230[a]	1073.4233
3.		62.41-62.83 (**8**)	996.3617[b]	996.3604
4.		61.83-62.23 (**9**)	1157.5185[a]	1157.5172
5.	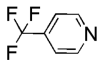	59.84-60.00 (**10**)	1165.3752[a]	1165.3718
6.		61.79-62.53 (**11**)	1030.3847[b]	1030.3811
7.		61.55-62.77 (**12**)	1111.5356[a]	1111.5341
8.		61.72--61.93 (**13**)	969.3607[b]	969.3597

*Reactions were performed in 1,4-dioxane using 0.01 mmol of the boranephosphonate dimer (**5**), 3 equiv of the NIS, and 10 equiv of the amines. Mass of the positively charged adducts and the corresponding ammonium species (a) or the mass of the protonated adducts (b) is indicated. R1: 5′-*O*-Dimethoxytrityl-2′-deoxythymidyl; R2: 3′-*O*-acetyl-2′deoxythymidyl.

Table 2. ODNs Having Pyridinium Boranephosphonate Modifications (py: Pyridinium Boranephosphonate; p: Phosphate

ODNs	Structure of ODNs[a]	Molecular Weight	
		Calculated	Observed
ODN 1	$T_{py}T$	621.499	621.1935
ODN 2	$T_{py}T_pT_pT_pT_pT_pT_pT_pT_pT_pT_pT_pT_pT_pT_pT_pT_pT_pT_pT_pT$	6399.242	6399.3912
ODN 3	$T_pT_pT_pT_pT_pT_pT_pT_pT_pT_pT_pT_{py}T_pT_pT_pT_pT_pT_pT_pT_pT_pT$	6399.242	6399.0791
ODN 4	$T_{py}T_pT_pT_pT_pT_pT_pT_pT_pT_pT_pT_pT_pT_pT_pT_pT_pT_pT_pT_pT_{py}T$	6478.312	6478.0219
ODN 5	$T_{py}T_{py}T_pT_pT_pT_pT_pT_pT_pT_pT_pT_pT_pT_pT_pT_pT_pT_pT_pT_{py}T_{py}T$	6630.452	6629.6827
ODN 6	$T_{py}T_{py}T_{py}T_pT_pT_pT_pT_pT_pT_pT_pT_pT_pT_pT_pT_pT_pT_pT_{py}T_{py}T_{py}T$	6774.4078	6774.2861

data, the similar chemical shifts of the BH_2 protons in the ^{11}B decoupled ^{1}H NMR spectra of **6** and **13** (2.83 and 2.55 ppm respectively, Figure S16) indicate a similar degree of delocalization of the positive charge over the aromatic system in both cases and support the reaction occurring at N3. Lastly, we found that simple tertiary amines such as trimethylamine and diisopropylethylamine were not suitable substrates for this reaction.

$[Pyr–I]^+I^-$ complexes have been studied in the literature not only for their conductive properties[10] but also in relation to halogen bonding stabilized molecular species.[11] In the present reaction, we speculate that the initial oxidation of a hydride on the BH_3 group proceeds with a concurrent substitution by the pyridinium moiety (Scheme 1). Such a concerted mechanism would explain the substitution occurring at the boron atom instead of phosphorus, which is observed

DOI: 10.1021/acs.joc.6b02599
J. Org. Chem. 2017, 82, 1420−1427

Scheme 1. Proposed Scheme for the Observed Reaction of Boranephosphonate Diesters with Pyridine

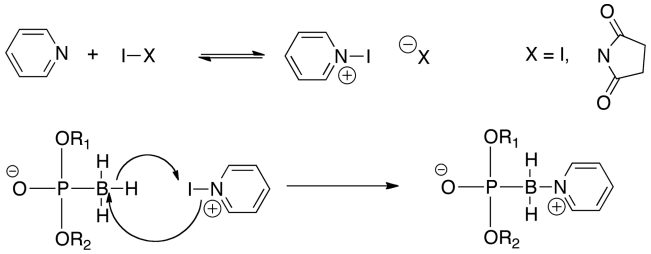

when the reaction occurs with iodine in the absence of pyridine.[7] The observation of slower reactivity at higher amounts of pyridine is consistent with the formation of complexes such as $[Pyr–I–Pyr]^+$ which are reported in the literature[11] and are less reactive. Lastly, the superior reactivity of *N*-iodosuccinimide, where the counterion to the $[Pyr–I]^+$ is a weaker coordinating succinimide anion, is also supportive of $[Pyr–I]^+$ being the reactive species.

Synthesis of Oligonucleotides Containing Pyridinium Boranephosphonate Linkages. Starting from boranephosphonate DNA (bpDNA), we further explored whether this reactivity could be used for the synthesis of DNA having these novel pyridinium boranephosphonate internucleotide linkages. The general approach we followed was as follows: (1) Synthesize 2′-deoxyoligothymidines having boranephosphonate diester linkages at specific sites. (2) Introduce pyridinium boranephosphonate by reacting the solid support bound bpDNA with NIS and pyridine. (3) Deprotect and cleave the ODN from the solid support using ammonium hydroxide.

Initially, a resin-bound 2′-deoxydithymidine containing a boranephosphonate diester linkage was treated with a solution of 0.1 M NIS in pyridine (ODN 1, Table 2). Upon cleavage and LCMS analysis, we found that the desired dimer containing a pyridinium boranephosphonate linkage was produced in near quantitative yield. We further carried out similar reactions on 21-mers of 2′-deoxyoligothymidine containing a single boranephosphonate diester linkage at the 5′ end or in the middle of the sequence (Table 2, ODNs 2 and 3) as well as oligomers containing two, four, or six boranephosphonate diester linkages (Table 2, ODNs 4, 5, and 6, respectively). In each case, synthesis of the corresponding pyridinium boranephosphonates proceeded efficiently. Analysis of the crude reaction mixtures by LCMS and ^{31}P NMR revealed the formation of the expected products in good yields. Table 2 lists the observed molecular weights for ODNs 1–6 as found by LCMS. Figure 3 shows a typical result as observed for ODN 6 (LCMS and ^{31}P NMR).

Cell Uptake of DNA Containing Pyridinium Boranephosphonate Internucleotide Linkages. In order to determine if pyridinium boranephosphonate containing oligonucleotides are taken up by cells, we synthesized the fluorescein-labeled ODNs 7, 8, 9, and 10 and carried out fluorescent-assisted cell sorting (FACS). Hela cells were cultured in media containing ODNs 7, 8, 9, and 10 for 24 h followed by removal of the media and thorough washing of the cells. Analysis by flow cytometry revealed enhanced uptake of these oligonucleotides with respect to the unmodified dT_{21} DNA control (Figure 4). The percentage of cells containing the fluorescein signal was found to increase with the number of pyridinium boranephosphonate linkages

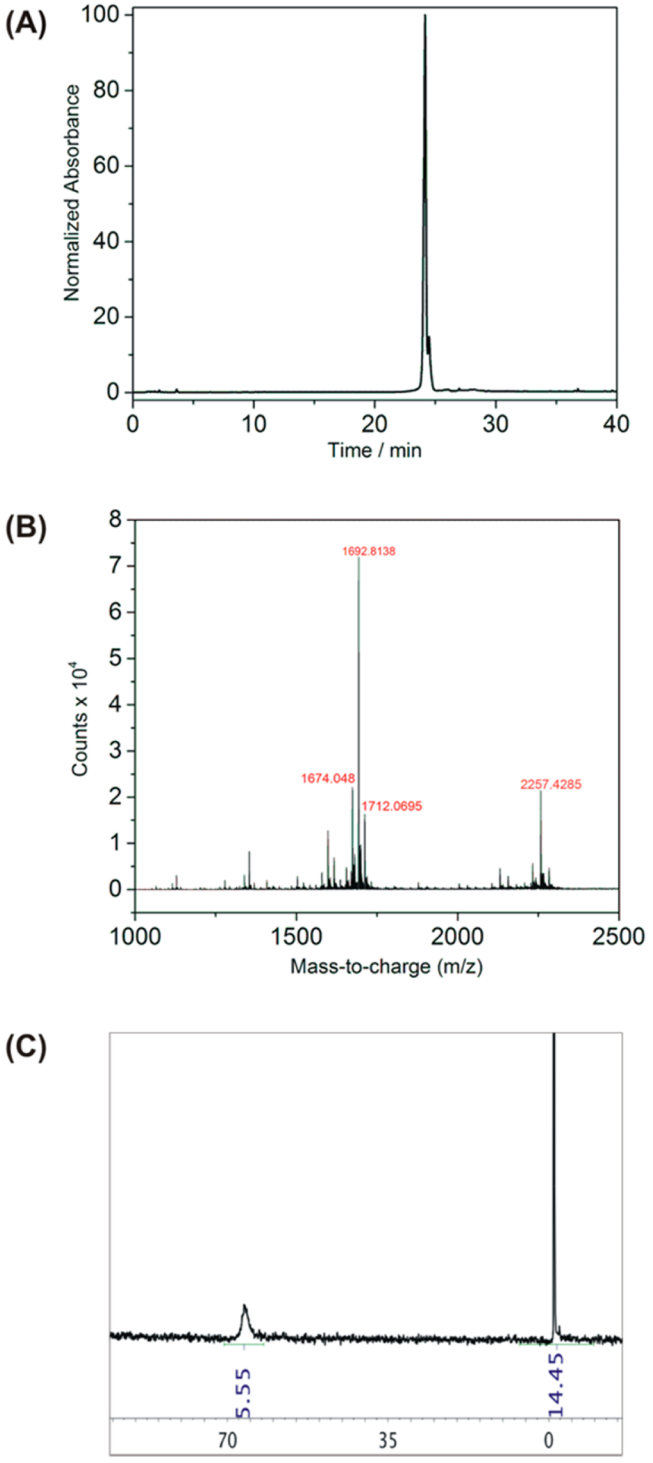

Figure 3. Diode array detector chromatogram monitored at 254 nm (A) and extracted mass spectrum (B) obtained from the LCMS analysis of ODN 6. The theoretical −4 and −3 charged peaks for the expected product are 1692.61 and 2257.53, respectively. (C) ^{31}P NMR of ODN 6.

present within each oligonucleotide as well as with the concentration of the oligomers added. Comparison of the uptake by ODNs 9 and 10 also revealed that the distribution of the pyridinium boranephosphonate linkages within the oligomers did not have a significant effect on the degree of uptake. We further analyzed the uptake by laser scanning confocal microscopy. Hela cells grown in glass-bottomed cell

DOI: 10.1021/acs.joc.6b02599
J. Org. Chem. 2017, 82, 1420–1427

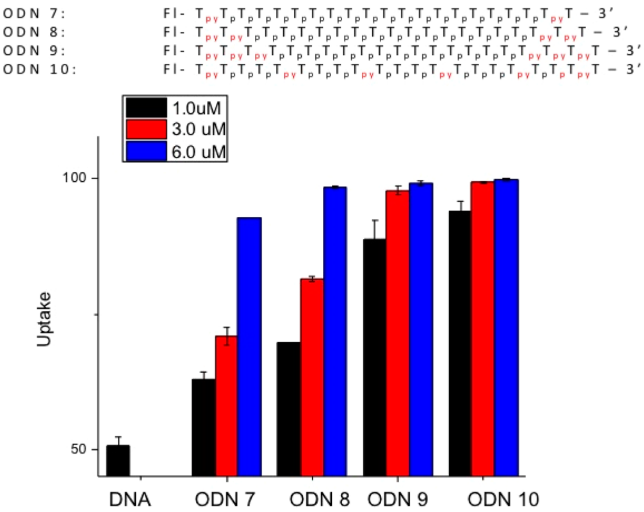

Figure 4. Uptake of DNA oligonucleotides containing pyridinium boranephosphonate internucleotide linkages by Hela cells. The bar graph presents the percentage of the total cells analyzed per experiment that showed positive uptake of oligonucleotide.

culture dishes were incubated with media containing 50 nM (Figure 5), 100 nM (Figure S17), and 1 μM (Figure S18) of ODN 10 for 16 h. After the cells were washed with PBS and cellular DNA was stained with the cell-permeable dye Hoechst 33258, live cell imaging was carried out. A fluorescein signal (green in Figure 5) indicating positive uptake was seen in all of the cells observed even at the lowest concentration of ODN 10. These experiments were carried out in the absence of lipid-based transfection agents.

Reduction of Metal Ions by Pyridinium Boranephosphonates. Boranephosphonate diesters readily reduce metal ions such as Au^{3+}, Ag^{+}, and Pt^{2+} at room temperature to produce the corresponding metallic nanoparticles.[5] In contrast, we found that pyridinium boranephosphonate dinucleotides had lower oxidation potentials. Figure 6 and Figure S19 show a comparison of the increase in the surface plasmon resonance bands for gold and platinum nanoparticles that form upon reduction by 5′-*O*-dimethoxytrityl-2′-deoxythymidyl 3′-*O*-acetyl-2′-deoxythymidyl boranephosphonate (**5**) and 5′-*O*-dimethoxytrityl-2′-deoxythymidyl 3′-*O*-acetyl-2′-deoxythymidylpyridinium boranephosphonate (**6**) at room temperature. In each case, the reduction by the pyridinium boranephosphonate derivative was much slower. Moreover, we found that **6** was completely unreactive toward Ag^{+} (data not shown), which has a lower reduction potential than Au^{3+} and Pt^{2+}. We have previously used the reductive properties of boranephosphonates for the construction of metallic nanostructures templated by DNA assemblies. Thus, the ability to modulate the reductive properties of boranephosphonates through substitution with pyridines has the potential for allowing deposition of nanoparticles composed of different metals onto DNA nanostructures in order to tailor plasmonic properties. Such multimetallic nanoparticles[12] have attracted interest in many fields such as catalysis, plasmonics, electronics and magnetics.

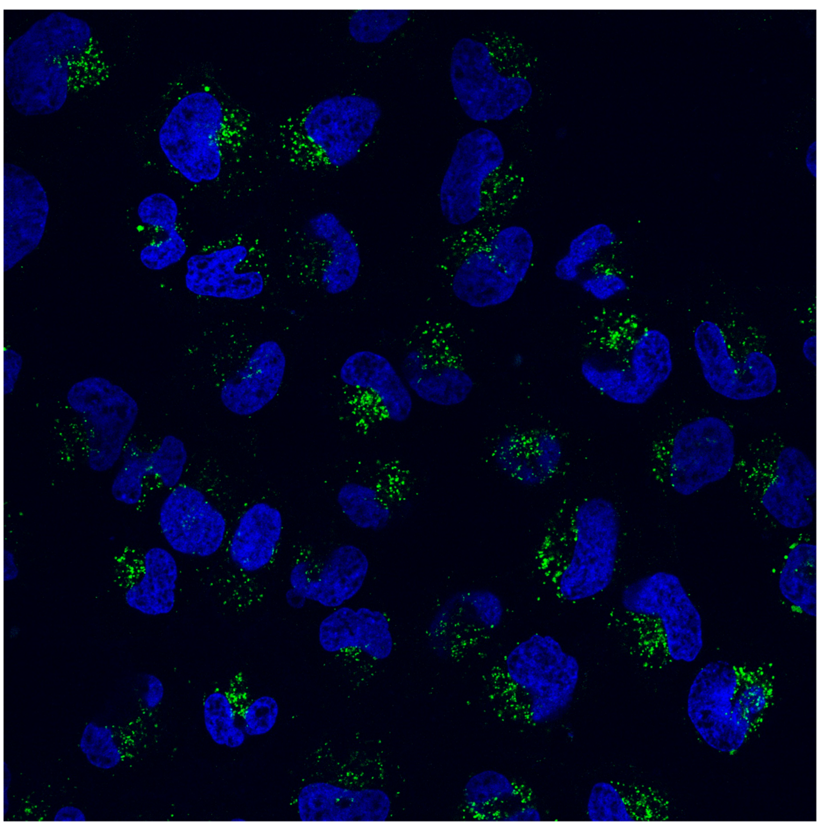

Figure 5. Laser scanning confocal microscopy image (100× magnification) of live Hela cells treated with 50 nM ODN10. The fluorescein signal is shown in green, while the DNA stained with Hoechst 33258 dye is shown in blue.

DOI: 10.1021/acs.joc.6b02599
J. Org. Chem. 2017, 82, 1420−1427

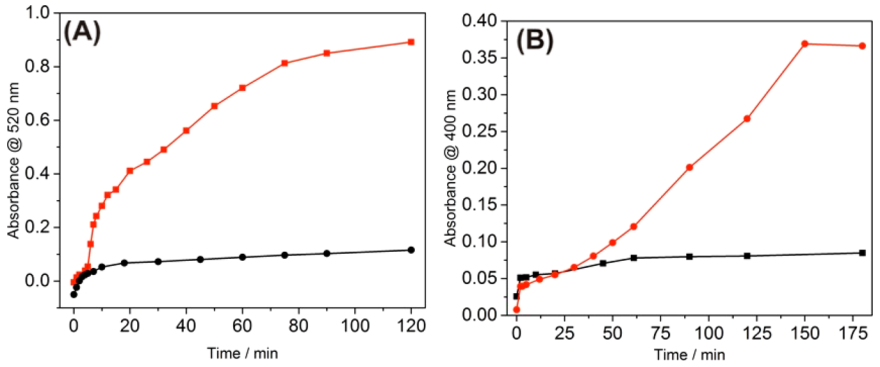

Figure 6. Growth of the surface plasmon band for gold (A) and platinum (B) nanoparticles upon reduction of Au^{3+} and Pt^{2+} ions by boranephosphonate dithymidine (**5**) (red traces) or pyridinium boranephosphonate dithymidine (**6**) (black traces) over time. Absorbance of nanoparticles was monitored at 520 nm for gold and 400 nm for platinum.

CONCLUSIONS

We have discovered a new reaction pathway whereby boranephosphonate diesters are converted to pyridinium boranephosphonate (and certain other amine boranes) by substitution of a borane hydride with a pyridinium or amine moiety. We were able to use this reactivity to prepare DNA oligomers having a novel backbone modification that showed enhanced uptake into Hela cells. These compounds also demonstrate lower oxidative potential with respect to the parent boranephosphonate diester. Current work is ongoing in our laboratory that is focused on using this reactivity for attaching pyridine-based metal complexes to DNA at internucleotide boranephosphonate linkages.

EXPERIMENTAL SECTION

General Methods. NMR experiments were carried out on a 400 MHz NMR spectrometer. Chemical shifts are given in ppm with positive shifts downfield. All ^{1}H and ^{13}C chemical shifts were referenced relative to the signal from residual protons of a lock solvent (CD_2Cl_2). For ^{1}H and ^{13}C, 5.32 and 54.00 ppm were used, respectively. HRMS spectra of low molecular weight compounds were recorded on a Q-TOF LCMS. DNA oligonucleotides were analyzed by LCMS that contained a UPLC instrument coupled to a Q-TOF spectrometer. A C18 column was used with a gradient of 0–100% of buffer B in 50 min with a flow rate of 0.2 mL/min at 75 °C (buffer A was a 1:80:9.5:9.5 mixture of 500 mM dibutylammonium acetate/water/2-propanol/acetonitrile and buffer B was a 1:10:44.5:44.5 mixture of 500 mM dibutylammonium acetate/water/ 2-propanol/acetonitrile).

Synthesis. *3′-O-(1,1-Dimethylcyanoethyl)boranephosphonate-5′-O-dimethoxytrityl-2′-deoxythymidine (**1**).* 3′-*O*-[Bis(1,1-dimethylcyanoethyl)phosphite]-5′-*O*-dimethoxytrityl-2′-deoxythymidine (1.1 g, 1.42 mmol) was dissolved in 40 mL of CH_2Cl_2 and dimethyl sulfide–borane complex (1.6 mmol) was added in a dropwise manner. The mixture was stirred for 20 min at room temperature, and 2 mL of methanol was added to quench excess borane. The reaction mixture was then evaporated to dryness under reduced pressure. The residue was resuspended in 20 mL of 2.0 M ammonia in methanol and stirred overnight at room temperature followed by evaporation of the solvent and ammonia under reduced pressure. This compound was dried under high vacuum and used without further purification. The compound was obtained as a white solid (0.85 g, 88%). ^{1}H NMR (CD_2Cl_2): δ 1.41, 1.44 (3H, each d), 1.50 (3H, d), 1.58 (3H, d), 2.33–2.64 (2H, m), 2.85 (2H, s), 3.33–3.51 (2H, m), 3.82 (6H, s), 4.30 (1H, m), 5.14 (1H, m), 6.40 (1H, m), 6.88 (4H, m), 7.25–7.37 (7H, m). 7.47 (2H, m), 7.58 (1H, m), 8.34 (1H, s). ^{31}P NMR (CD_2Cl_2): δ 91.52. ^{11}B NMR (CD_2Cl_2): δ −38.54.

*3′-O-(1,1-Dimethylcyanoethyl)pyridiniumboranephosphonate-5′-O-dimethoxytrityl-2′-deoxythymidine (**3**).* 3′-*O*-Boranephosphonate-5′-*O*-dimethoxytrityl-2′-deoxythymidine (**1**) (200 mg) was dissolved in 9.0 mL of tetrahydrofuran and 3.0 mL pyridine to which 126.5 mg of I_2 was added. After being stirred for 3 h at room temperature, the reaction mixture was diluted with 50 mL of methylene chloride. The organic layer was washed twice with a 0.1 M solution of sodium thiosulfate and once with brine, dried over sodium sulfate, and evaporated to dryness. The compound was purified by silica gel column chromatography with a gradient of 100% chloroform to a 9:1 chloroform/methanol mixture. The silica gel was neutralized by preparing a slurry with the starting eluant mixture containing an additional 5% triethylamine. After the silica gel slurry was poured, the column was washed with two column volumes of the starting eluant mixture containing no triethylamine. Compound **3** was obtained as a white solid (185 mg, 82% yield). ^{1}H NMR (CD_2Cl_2): δ 1.57–1.63 (6H, m), 1.68 (3H, d), 2.47–2.64 (2H, m), 2.94 (2H, s), 3.54 (2H, m), 3.95 (6H, s), 4.31 (1H, m), 5.5 (1H, m), 6.46–6.51 (1H, m), 7.01–7.03 (4H, m), 7.40–7.43 (1H, m), 7.46–7.51 (6H, m), 7.59–7.62 (2H, m), 7.7 (1H, dd), 7.82–7.89 (2H, p), 8.28 (1H, m), 8.74–8.83 (2H, m), 9.6 (1H, d). ^{31}P NMR (CD_2Cl_2): δ 60.92 (broad). ^{11}B NMR (CD_2Cl_2): δ −12.66. ^{13}C NMR (CD_2Cl_2): δ 12.08, 12.13, 28.57, 28.6, 28.68, 28.7, 29.0, 32.86, 32.89, 40.2, 40.3, 55.8, 64.2, 73.77, 73.84, 73.9, 74.0, 77.3, 77.35, 77.40, 77.5, 85.0, 85.78, 85.82, 85.94, 85.99, 87.5, 111.67, 111.70, 113.7, 113.8, 118.2, 118.3, 126.77, 126.79, 126.83, 126.9, 127.6, 128.5, 128.7, 128.8, 130.71, 130.73, 135.9, 136.00, 136.05, 136.13, 136.2, 141.9, 145.1, 145.2, 148.6, 148.6, 148.6, 148.7, 151.2, 159.4, 164.4 HRMS (ESI-qTOF): $(M + Et_3NH^+)^+$ calcd for $C_{47}H_{62}BN_5O_9P$ 882.4378, found 882.4377.

*3′-O-Bis(1,1-dimethylcyanoethyl)borane-d_3-phosphonate-5′-O-dimethoxytrityl-2′-deoxythymidine (**2**).* To a solution of 3′-*O*-bis(1,1-dimethylcyanoethyl) phosphite-5′-*O*-dimethoxytrityl 2′-deoxythymidine (800 mg) in 20 mL of anhydrous tetrahydrofuran was added 2 equiv of borane-d_3–THF complex, and the reaction mixture was stirred for 30 min at room temperature. At this point, complete conversion to the boronated product occurred as determined by a single broad peak in the ^{31}P NMR spectrum at 109 ppm. Methanol (2 mL) was added to quench the excess borane-d_3, and the reaction mixture evaporated to dryness. Ammonia in methanol solution (20 mL, 2.0 M) was added to this crude mixture, which was stirred overnight. ^{31}P NMR showed complete conversion to the diester (broad peak at 93 ppm). The ammonia was evaporated under reduced pressure, and the product was used for the next step.

*3′-O-(1,1-Dimethylcyanoethyl)pyridiniumborane-d_3-phosphonate-5′-O-dimethoxytrityl-2′-deoxythymidine (**4**).* The procedure was exactly as described for the synthesis of **3**. ^{1}H NMR (CD_2Cl_2): δ 1.42 (6H, m), 1.52 (3H, d), 2.32–2.42 (2H, m), 2.94 (2H, m), 3.36 (2H, m), 3.77 (6H, s), 4.13 (1H, m), 5.12 (1H, m), 6.30 (1H, m), 6.84 (4H, m), 7.24 (1H, m), 7.28–7.33 (6H, m), 7.4–7.45 (2H, m), 7.51 (1H, m), 7.67 (2H, p), 8.09 (1H, t, pyridinium-*para*), 8.60 (2H,

DOI: 10.1021/acs.joc.6b02599
J. Org. Chem. 2017, 82, 1420–1427

m). ^{31}P NMR (CD_2Cl_2): δ 61.34. ^{11}B NMR (CD_2Cl_2): δ −10.60. ^{13}C NMR (CD_2Cl_2): δ 11.5, 28.4, 32.3, 45.6, 54.00, 63.6, 84.4, 85.3, 86.9, 113.2, 126.3, 127.0, 128.0, 128.1, 130.1, 135.5, 141.2, 144.5, 148.0, 150.4, 158.8, 163.5. HRMS (ESI-QTOF): $(M + Et_3NH^+)^+$ calcd for $C_{47}H_{60}D_2BN_5O_9P$ 884.4503, found 884.4484.

*5′-O-Dimethoxytrityl-2′-deoxythymidyl 3′-O-acetyl-2′-deoxythymidylpyridiniumboranephosphonate (**6**).* 5′-*O*-Dimethoxytrityl-2′-deoxythymidyl 3′-O-acetyl-2′-deoxythymidyl boranephosphonate (**5**) (0.5 mmol, 440 mg) was dissolved in 20 mL of anhydrous dioxane along with 5 mmol (395 mg) of pyridine followed by 1.5 mmol (338 mg) of NIS. The mixture was allowed to stir at room temperature overnight and quenched by dilution with 100 mL of ethyl acetate and extraction of the organic layer three times with 75 mL water. The organic layer was dried over Na_2SO_4 and evaporated to dryness. The product was purified by silica gel column chromatography. The silica gel was neutralized by preparing the silica gel in $CHCl_3$ containing 5% triethylamine. After the silica gel slurry was poured, the column was washed with two column volumes of the starting eluant mixture containing no triethylamine. The compound was purified using a gradient of 100% $CHCl_3$ to 9:1 $CHCl_3/CH_3OH$ to yield 450 mg of a white solid (92% yield). ^{1}H NMR (CD_2Cl_2): δ 1.41, 1.45 (3H, d each), 1.92, 1.94 (3H, d each), 2.09, 2.10 (3H, s each), 2.17−2.56 (4H, m), 3.38 (2H, m), 3.795 and 3.805 (6H, 2 s each), 3.87−4.28 (4H, m), 5.26 (2H, m), 6.35 (2H, m), 6.87 (4H, m), 7.24−7.36 (7H, m), 7.44 (2H, m), 7.54 (1H, m), 7.62−7.69 (2H, m), 7.75 (1H, t), 8.14 (1H, m), 8.64 (2H, m), 10.22 (2H). ^{13}C NMR (CD_2Cl_2): δ 9.4, 11.55, 11.61, 12.2, 12.3, 20.79, 20.82, 29.1, 30.6, 37.2, 45.8, 55.22, 55.24, 62.6, 62.8, 63.57, 63.63, 73.5, 73.8, 74.9, 75.1, 83.6, 84.29, 84.33, 84.5, 84.6, 85.1, 85.4, 86.90, 86.94, 111.20, 111.22, 111.35, 111.41, 113.2, 126.40, 126.43, 126.50, 126.53, 127.0, 128.0, 128.10, 128.13, 130.13, 135.29, 135.36, 135.42,135.5, 135.6, 141.6, 141.7, 144.5, 147.90, 147.97, 148.02, 150.9, 158.8, 164.27, 164.32, 164.35, 170.3, 170.4, ^{31}P NMR (CD_2Cl_2): δ 61.33. ^{11}B NMR (CD_2Cl_2): δ −14.41. HRMS (ESI-QTOF): $(M + Et_3NH^+)^+$ calcd for $C_{54}H_{69}BN_6O_{14}P$ 1067.4702, found 1067.4688. This mass includes a triethylammonium ion due to its isolation from column chromatography, thus the difference from the mass reported in Table 1.

*Compound **11**.* The procedure used was as described for the synthesis of **6**. Starting from 0.44 g of **5**, 0.32 g of **11** was obtained as a white solid (65% yield). ^{1}H NMR (CD_2Cl_2): δ 1.39 (3H, s), 1.82 (3H, s), 2.09, 2.10 (3H, s each), 2.16−2.55 (4H, m), 2.88, 2.90 (3H, s each), 3.26 (1H, s), 3.41 (1H, s), 3.79, 3.80 (6H, s each), 3.86−4.09 (2H, m), 4.21 (2H, s broad), 5.12−5.31 (2H, m), 6.32 (2H, m), 6.84, 6.86 (4H, s each), 7.25−7.33 (7H, m), 7.42 (2H, t), 7.50 (1H, m), 7.56 (1H, m), 7.81 (1H, q), 8.01 (1H, m), 8.18 (1H, m), 8.63 (1H, s (broad)), 8.85−8.98 (2H, m), 9.44 (2H, m). ^{13}C NMR (CD_2Cl_2): δ 9.8, 11.5, 11.6, 12.0, 12.1, 19.5, 20.77, 20.80, 37.3, 37.4, 39.5, 39.8, 46.1, 55.21, 55.22, 62.4, 62.5, 62.9, 63.6, 73.2, 73.3, 73.9, 74.0, 75.0, 83.5, 83.6, 83.7, 84.3, 84.5, 84.7, 85.2, 85.5, 86.88, 86.90, 111.04, 111.08, 111.2, 111.3, 113.2, 122.1, 124.7, 124.8, 125.01, 125.05, 127.0, 127.9, 128.1, 128.6, 129.10, 129.12, 130.09, 130.12, 132.59, 132.61, 135.29, 135.32, 135.39, 135.44, 135.6, 141.77, 141,81, 144.5, 150.65, 150.71, 150.74, 151.4, 151.5, 154.1, 158.76, 158.78, 164.07, 164.12, 164.15, 170.2, 170.4. ^{31}P NMR (CD_2Cl_2): δ 62.2, ^{11}B NMR (CD_2Cl_2): δ −15.4. HRMS (ESI-QTOF): $(M + Et_3NH^+)^+$ calcd for $C_{59}H_{73}BN_6O_{14}P$ 1131.5015, found 1131.4996. This mass includes a triethylammonium ion due to its isolation from column chromatography, thus the difference from the mass reported in Table 1.

*Compound **13**.* The procedure used was as described for the synthesis of **6**. Starting form 0.44 g of **5**, 0.392 g of **13** was obtained as a white solid (81% yield). ^{1}H NMR (CD_2Cl_2): δ 1.41, 1.45 (3H,s each), 1.91, 1.93 (3H, s each), 2.08, 2.10 (3H, s each), 2.14−2.45 (4H, m), 2.55 (2H, m), 3.4 (2H, m), 3.80 (9H, m), 3.91 (1H, m), 4.19 (3H, m), 5.27 (2H, m), 6.35 (2H, m), 6.87 (dd, 4H), 7.01−7.15 (2H, m), 7.24−7.35 (7H, m), 7.45 (2H, m), 7.56 (1H, d), 7.68 (1H, d), 8.19 (1H, d). ^{13}C NMR (CD_2Cl_2): δ 9.5, 11.56, 11.62, 12.2, 12.3, 20.81, 20.84, 35.2, 35.3, 37.2, 37.3, 39.5, 39.9, 40.9, 45.9, 55.23, 55.24, 62.26, 62.33, 62.57, 62.63, 63.6, 63.7, 73.6, 73.70, 73.73, 73.80, 75.1, 75.4, 83.65, 83.72, 84.4, 84.5, 84.6, 85.13, 85.17, 85.41, 85.45, 86.66, 86.93, 111.12, 111.16, 111.30, 111.34, 113.19, 121.9, 122.1, 127.0, 127.1, 127.2, 127.96, 128.10, 128.14, 130.15, 135.3, 135.4, 135.5, 135.6, 135.69, 135.74, 138.06, 138.12, 138.18, 144.6, 150.9, 151.0, 158.74, 158.76, 164.31, 164.34, 164.40, 164.42, 170.3, 170.5. ^{31}P NMR (CD_2Cl_2): δ 64.5. ^{11}B NMR (CD_2Cl_2): δ −17.7. HRMS (ESI-QTOF): $(M + Et_3NH^+)^+$ calcd for $C_{53}H_{70}BN_7O_{14}P$ 1070.4811, found 1070.4796.

Solid-Phase Pyridinium Boranephosphonate DNA Synthesis. ODNs containing boranephosphonate linkages were synthesized as described previously[4] on a 0.2 μmol scale on a highly cross-linked polystyrene resin using 5′-dimethoxytrityl-2′-deoxythymidine-3′-*O*-cyanoethyl-*N*,*N*-diisopropylphosphoramidite. Following synthesis, the cyanoethyl protection was removed by treatment of the resin-bound oligonucleotide with a solution of 20% diethylamine in acetonitrile for 20 min. The resin was transferred to a glass vial, and pyridinium boranephosphonate linkages were generated by treatment with a solution of *N*-iodosuccinamide (0.1M) in anhydrous pyridine for 24 h. The resin was washed 4−5 times with 2 mL aliquots of acetonitrile by repeated centrifugation, removal of the supernatant with a pipet, and addition of fresh solvent. The oligonucleotide was then cleaved from the resin by adding 37% ammonium hydroxide in water followed by incubation for 30 min at room temperature. After removal of the resin by filtration, the oligonucleotide solution was evaporated to dryness in a SpeedVac, and the product was redissolved in water and used for subsequent analyses.

Cell Uptake Studies. *Flow Cytometry.* 8×10^4 HeLa cells/well (12-well plates) were incubated in DMEM containing 10% fetal bovine serum, penicillin (100 U/mL), and streptomycin (100 U/mL) for 24 h. The concentration of 5′-fluorescein-labeled ODN dissolved in water was measured by UV spectroscopy. The medium was removed, and the cells were transfected with the appropriate ODN in DMEM to give the required final concentration. The cells were then incubated at 37 °C for 16 h. After incubation, the medium was removed from the wells, and and cells were washed three times with PBS. Cells were then treated for 3 min at 37 °C with a prewarmed solution of trypsin−EDTA (1×) until all cells became detached from the plates. The cells from each plate were then suspended in 1 mL of PBS and pelleted by centrifugation at 1000 rpm for 5 min. The pellets were washed and resuspended in PBS and kept on ice until they were analyzed by flow cytometry. Flow cytometric data on at least 10000 cells per sample were acquired on a flow-cytometer equipped with a single 488 nm argon laser, 530/40 nm emission filter. Raw flow cytometry data was manipulated and visualized using Summit 4.3 software. Fluorescence intensity of the 5′-fluorescein tag was analyzed for cells presenting higher fluorescence than the background. The background was defined as the autofluorescence of cells.

Laser-Scanning Confocal Microscopy. Fluorescence microscopy was done on a Nikon A1R laser-scanning confocal microscope using a 100× oil immersion objective and an environment control chamber set at 37 °C and an atmosphere of 5% CO_2. Hela cells were incubated in a 24-well glass-bottomed cell culture plate (40000 cells/well) in DMEM containing 10% fetal bovine serum, penicillin (100 U/mL), and streptomycin (100 U/mL) for 24 h. The medium in each well was then replaced by 500 μL of fresh medium containing various amounts of ODN 10, and the cells were incubated for a further 16 h. At this point, the medium was removed, and the cells were washed three times with PBS, and 1 mL of phenol red free DMEM containing 10% fetal bovine serum, penicillin (100 U/mL), and streptomycin (100 U/mL) was added. Hoechst 33258 was added at a concentration of 10 ng/mL to each well, and the cells were incubated at 37 °C for 30 min followed by imaging. Lasers (488 and 405 nm) were used to excite fluorescein and Hoechst 33258, respectively.

DOI: 10.1021/acs.joc.6b02599
J. Org. Chem. 2017, 82, 1420−1427

■ ASSOCIATED CONTENT

Supporting Information

The Supporting Information is available free of charge on the ACS Publications website at DOI: 10.1021/acs.joc.6b02599.

^{1}H NMR, ^{13}C NMR, and HRMS traces of compounds **3**, **6**, **11**, and **14**. ^{31}P NMR spectra corresponding to Figure 2B and UV−vis spectra from metal reduction experiments (PDF)

■ AUTHOR INFORMATION

Corresponding Author

*E-mail: marvin.caruthers@colorado.edu.

ORCID

Subhadeep Roy: 0000-0002-8297-8541

Notes

The authors declare no competing financial interest.

■ ACKNOWLEDGMENTS

This research was supported by the University of Colorado. The imaging work was performed at the BioFrontiers Institute Advanced Light Microscopy Core. Laser scanning confocal microscopy was performed on a Nikon A1R microscope acquired by the generous support of the NIST−CU Cooperative Agreement Award No. 70NANB15H226.

■ REFERENCES

(1) Li, P.; Sergueeva, Z.; Dobrikov, M.; Shaw, B. R. *Chem. Rev.* **2007**, *107*, 4746−4796.

(2) Shimizu, M.; Saigo, K.; Wada, T. *J. Org. Chem.* **2006**, *71*, 4262−4269.

(3) Matsumura, F.; Oka, N.; Wada, T. *Org. Lett.* **2008**, *10*, 1557−1560.

(4) Roy, S.; Olesiak, M.; Shang, S.; Caruthers, M. H. *J. Am. Chem. Soc.* **2013**, *135*, 6234−6241.

(5) Roy, S.; Olesiak, M.; Padar, P.; McCuen, H.; Caruthers, M. H. *Org. Biomol. Chem.* **2012**, *10*, 9130−9133.

(6) Russell, C.; Roy, S.; Ganguly, S.; Qian, X.; Caruthers, M. H.; Nilsson, M. *Anal. Chem.* **2015**, *87*, 6660−6666.

(7) Paul, S.; Roy, S.; Monfregola, L.; Shang, S.; Shoemaker, R.; Caruthers, M. H. *J. Am. Chem. Soc.* **2015**, *137*, 3253−3264.

(8) Ferry, A.; Guinchard, X.; Retailleau, P.; Crich, D. *J. Am. Chem. Soc.* **2012**, *134*, 12289−12301.

(9) Denniston, M. L.; Chiusano, M.; Brown, J.; Martin, D. R. *J. Inorg. Nucl. Chem.* **1976**, *38*, 379−382.

(10) Tassaing, T.; Besnard, M. *J. Phys. Chem. A* **1997**, *101*, 2803−2808.

(11) Carlsson, A. C.; Mehmeti, K.; Uhrbom, M.; Karim, A.; Bedin, M.; Puttreddy, R.; Kleinmaier, R.; Neverov, A. A.; Nekoueishahraki, B. *J. Am. Chem. Soc.* **2016**, *138*, 9853−9863.

(12) Chen, P.; Liu, G.; Zhou, Y.; Brown, K. A.; Chernyak, N.; Hedrick, J. L.; He, S.; Xie, Z.; Lin, Q.; Dravid, V. P.; O'Neill-slawecki, S. A. O.; Mirkin, C. A. *J. Am. Chem. Soc.* **2015**, *137*, 9167−9173.

DOI: 10.1021/acs.joc.6b02599
J. Org. Chem. 2017, 82, 1420−1427